

Microfluidics for Greener Flow-Based Colorimetric Analysis of Phosphate and Cinnarizine

Natthaya Siangdee, Panumas Yaemmak, Suwimon Chaohuaimak,
Thuan Hoa Nguyen, Duy Hien Nguyen, Chawin Srisomwat, Napaporn Youngvises*

*Department of Chemistry, Faculty of Science and Technology, Thammasat University,
Pathum Thani 12120, Thailand*

Received 28 May 2024; Received in revised form 20 October 2024

Accepted 7 November 2024; Available online 27 December 2024

ABSTRACT

Microfluidic systems are gaining popularity in analytical chemistry owing to their compact size, reduced reagent consumption, and alignment with the principles of green analytical chemistry. In this study, novel microfluidic systems were successfully employed for the determination of phosphate in surface water samples, and cinnarizine in tablet formulations. The three-dimensional lab on a chip (3D LOC) was designed and microfabricated on polymethyl methacrylate (PMMA) in a rectangular figure similar to the conventional flow-through cell. The outstanding is not only a space for the solution to flow through the cell in the spectrophotometer but also a coil for the reaction of sample and reagent to achieve the compact system and enhancement of chemical analysis performance. The 3D LOC was applied for the determination of phosphate in water samples and cinnarizine in tablet dosage forms incorporating the reverse flow injection analysis (r-FIA) with colorimetric detection. The result obtained linear ranges of phosphate is 0.010-2.0 mg P L⁻¹ with an R² of 0.9985, and those of cinnarizine were 10-150 mg L⁻¹ with an R² of 0.9963. These designs demonstrated excellent performance characterized by wide linear ranges, low detection limits, and good precision. The proposed microfluidic system holds significant potential to be a greener analytical chemistry.

Keywords: Cinnarizine; Flow-through-cell; Microfluidics; Phosphate; Three-dimension lab on a chip (3D LOC)

1. Introduction

Green Analytical Chemistry (GAC) is a branch of analytical chemistry that focuses on

developing and implementing sustainable and environmentally friendly practices in analytical processes. The primary goal of GAC

is to reduce the environmental impact of analytical methods by minimizing resource consumption, waste generation, and the use of hazardous chemicals [1, 2]. Microfluidics has become the technique that supports GAC by minimizing the size of a device system. It provides precise control over fluid flow, mixing, and reactions, leading it to be a valuable tool in various applications [3] such as analytical chemistry, biology [4], medicine [5-7], and environmental monitoring [8, 9]. There are several platforms for the microfluidic system, such as two- and three-dimensional platforms [10-17]. The role of the microchannel platform is not only to support greener analytical chemistry but also to reduce cost of the analysis. This technology is particularly well-suited for green analytical chemistry, where the focus is on using safer and more environmentally friendly reagents and methodologies [18]. The incorporation of microfluidic technology into r-FIA presents several advantages in reducing of sample/reagent volume, analysis times, and improving sensitivity and accuracy [19].

Phosphate is a critical analyte in environmental monitoring due to its impact on water quality and the ecosystem. An overabundance of phosphate in natural water causes pollution called eutrophication. The USEPA has set a recommended limit no more than 0.1 mg L^{-1} for total phosphorus in flowing waters, and 0.05 mg L^{-1} for total phosphates in streams flowing into lakes [20]. The predominant methods used for phosphate determination in natural water rely on spectrophotometric detection based on the phosphomolybdenum blue reaction [21]. This reaction generates a blue-colored product known as the phosphomolybdenum blue (PMB) complex, formed by the reaction between orthophosphate (o-PO_4^{3-}) and molybdate ions in an acidic medium, followed by the reducing agent. Spectrophotometry is the favorite method for phosphate determination due to its simplicity, ease of observation, sensitivity and compatibility with automated systems. Numerous studies have focused on developing colorimetric detection methods integrated with

automated flow-based systems for phosphate determination in natural water [22-26].

Cinnarizine, a pharmaceutical compound commonly used to treat vertigo and motion sickness, requires meticulous quantification in tablet formulations to ensure therapeutic efficacy and safety. Commercial cinnarizine tablets are formulated with 15, 25, 50, or 75 mg. Cinnarizine can be determined by several methods including high performance liquid chromatography (HPLC) as a confirmation technique [27, 28], thin-layer chromatography (TLC) [29, 30], UV-visible spectroscopy [31, 32], and chemiluminescence with flow injection analysis (FIA-CL) [33]. The British Pharmacopoeia 2020 [34] also utilized HPLC with C18 as an official method for assay of cinnarizine in tablets dosage form. Most methods require costly instrumentation. The chromatographic techniques are suitable for analyzing complex mixtures; however, they require long analysis time and skilled operators. While FIA-CL boasts high sensitivity, it relies on specialized detectors like photomultiplier tubes. Certain spectrophotometric methods for cinnarizine analysis involve the consumption of hazardous reagents.

In this research, we focused on the design and invention of a micro flow-through cell as a 3D LOC in operation to r-FIA with colorimetric detection, and utilizing it for the determination of phosphate in surface water samples, and cinnarizine in tablet dosage form, based on PMB reaction and oxidation by KMnO_4 in an acidic medium, respectively.

2. Materials and Methods

2.1 Reagent and chemicals

All chemicals and reagents used in this study were of analytical grade. Cinnarizine ($\text{C}_{26}\text{H}_{28}\text{N}_2$) and L-ascorbic acid ($\text{C}_6\text{H}_8\text{O}_6$) were purchased from Sigma-Aldrich, Germany. Ammonium molybdate tetrahydrate ($(\text{NH}_4)_6\text{Mo}_7\text{O}_{24} \cdot 4\text{H}_2\text{O}$) and potassium permanganate (KMnO_4) were obtained from Carlo Erba, Italy. Antimony potassium tartrate ($\text{KSbOC}_4\text{H}_4\text{O}_6 \cdot 0.5\text{H}_2\text{O}$), potassium chloride

(KCl) and sodium hydrogen carbonate (NaHCO_3) were provided by Ajax Finechem, Australia. Potassium dihydrogen phosphate (KH_2PO_4), ammonium chloride (NH_4Cl) and metal ions of Fe(III), Cu(II), Zn(II), Pb(II), Al(III), Ca(II) and Mn(II) for interference study were supplied by Merck, Germany. Finally, hydrochloric acid (37%), and sulfuric acid (99.8%) were purchased from QReC, New Zealand. The deionized water (ELGASTAT Option 3A, 13172 G, Elga Ltd., Bucks, England) was used throughout the experiment.

2.2 Design and fabrication of 3D LOC

The 3D LOC as shown in Fig. 1. was designed and microfabricated using CO_2 laser etching (Laser1325, CNCBro, China) on an opaque black polymethyl methacrylate (PMMA); its shape was a rectangular box (10 mm in width, 10 mm in length and 45 mm in height). The first part of the microchannel acted as a reaction coil (250 μm width, 500 μm depth, 260 mm length, and 80 μL capacity) with an etching rate of 60 mm s^{-1} at 30% power. The second part was a flow-through cell (10 mm pathlength and 2 mm diameter) with the etching rate of 4 mm s^{-1} at 89% power. This design of a microchannel network (b) was fabricated on two sides of the PMMA with 12 holes to bridge the channel on both sides. The microchannel was sealed using a thermal bonding process at 60°C for 6 min, forming a sandwiched structure

with two transparent PMMA pieces of 1 mm thickness, 10 mm width, and 45 mm height. The volume capacity of the flow through the cell (c) was 31 μL . The chip was connected to polytetrafluoroethylene (PTFE) tubing (ID 0.45 mm, OD 1.6 mm, VICI, Canada) at the inlet (a) and outlet(d).

The schematic diagram of the proposed method, which coupled the 3D LOC with a reverse flow injection analysis (r-FIA) system for phosphate determination in natural water and cinnarizine determination in tablet formulation is represented in Fig. 2. A simple reverse flow injection manifold consisted of a peristaltic pump, a six-port valve, and 3D LOC (same size as a conventional cuvette) inside the spectrophotometer. Samples and standard solution were delivered using a peristaltic pump (FIALab®, USA) with 0.89 mm id of polyvinyl chloride pump tubing (color code: orange/orange, ISMATEC, Switzerland) and then the colorimetric reagent was injected into the solution stream via a six-port valve and delivered into the 3D LOC, where the solution reacted within the microchannel network and flowed into the detection flow cell. Then, the absorbance of colored product was measured using a visible spectrophotometer (V-1200, MAPADA, China) with the M.Wave Professional 2.0 software program to plot a FIAGram and determine the peak height. Three replicate injections were carried out and analyzed for each standard/sample solution.

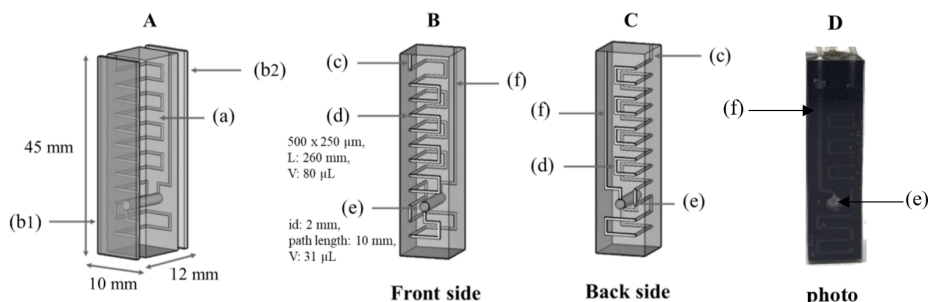


Fig. 1. The 3D LOC design (A) is presented, and the microchannel network within the chip is demonstrated. The 3D-LOC consisted of (a) an opaque black PMMA rectangular box, and two transparent PMMA pieces (b1 and b2). The front side (B) and back side (C) of 3D LOC show an inlet (c) (1.6 mm id); microchannel as a reaction coil (d) in a flow-cell; detection area (e) in cylindrical channel; and outlet (f) (1.6 mm id). The real photo of 3D LOC is also presented (D).

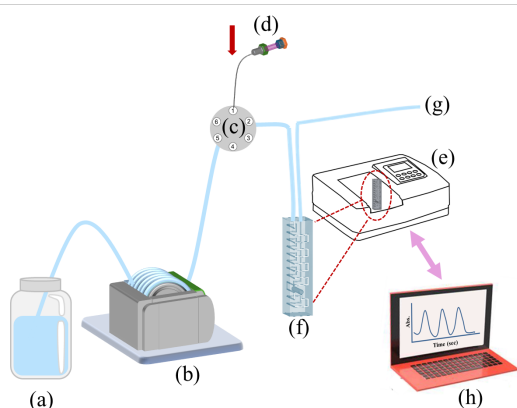


Fig. 2. The schematic of the 3D LOC in r-FIA system consisted of standard/sample (a); a peristaltic pump (b); an injection valve (c); a syringe containing reagent (d); a spectrophotometer (e), 3D LOC, waste (g), and computer (h).

2.3 Application for phosphate analysis

This system was prepared and evaluated based on the molybdenum blue reaction between PO_4^{3-} and ammonium molybdate in acid solution [21, 35]. The sequent reaction involved the reaction of o-PO_4^{3-} with molybdate ions in an acidic solution and formed a yellow 12-molybdophosphoric acid (12-PMA) complex. The reaction was carried out in an acidic solution containing ascorbic acid as a reducing agent, which concerted the complex into a blue colored PMB complex with maximum light absorption at wavelength 880 nm. Then, 3D LOC was applied for determination of PO_4^{3-} based on PMB reaction by injecting the combined reagent into the stream of PO_4^{3-} standard/sample solution, and monitoring light absorption at 880 nm. The 3D LOC cooperating to r-FIA is shown in Fig. 2. The FIAgram was monitored in absorbance value vs. time (sec); the signal of PO_4^{3-} (in absorbance value) was calculated by subtraction between the peak height of PO_4^{3-} and blank, whereas the blank peak was monitored by injection of combined reagent in the water stream. A 3-replicate injection was used throughout the experiment.

A stock standard solution of phosphate (100 mg P L⁻¹) was prepared using potassium

dihydrogen phosphate dissolved in deionized water. The working standard phosphate solution was kept in a plastic bottle and stored in a refrigerator. A mixed reagent was freshly prepared in 10.0 mL and made by sequentially mixing 5.0 mL of 4 mol L⁻¹ H₂SO₄, 1.5 mL of 10 mmol L⁻¹ ammonium molybdate tetrahydrate, 0.5 mL of 8 mmol L⁻¹ antimony potassium tartrate and 3.0 mL of 0.5 mol L⁻¹ reducing agent. Ascorbic solution was prepared by dissolving 4.40 g of ascorbic acid in 50.0 mL of deionized water.

In the optimization study, the effects of concentration of reagents and flow rate were studied using a univariate optimization by considering sensitivity of the measurement. The combined reagent consisted of 4 mol L⁻¹ H₂SO₄, 10 mmol L⁻¹ ammonium molybdate, 8 mmol L⁻¹ antimony tartrate and 0.5 mol L⁻¹ ascorbic acid; it was used as a starting condition for optimization, with a flow rate 1 mL min⁻¹ and 1.0 mg P L⁻¹ standard phosphate solution used throughout the optimization study.

This method was applied for determination of phosphate in surface water samples. Ten samples of surface water were collected at different areas in Thammasat University, Rangsit campus, Pathum Thani, Thailand. Each sample was filtered through filter paper (Whatman No.1) and stored in a plastic bottle. The samples were analyzed by the proposed system and compared to a batch method of PMB reaction using a visible spectrophotometer (V-1200, MAPADA, China) with a conventional cuvette (10.0 mm pathlength) [36]. The result was compared between the results of both methods by paired t-test at 95% confidence level.

2.4 Application for cinnarizine analysis

The 3D LOC was utilized for the determination of cinnarizine in tablet dosage form based on the oxidation reaction of cinnarizine by KMnO₄ in a r-FIA (Fig. 2) and the color of KMnO₄ was faded depending on the increasing concentration of standard cinnarizine, which was detected by the

spectrophotometer at 525 nm. The KMnO_4 was injected into the standard/sample stream.

A stock standard solution of cinnarizine ($1,000 \text{ mg L}^{-1}$) was prepared daily in 0.1 mol L^{-1} hydrochloric acid. The standard cinnarizine solution was diluted to construct a standard calibration graph in the range of $1.0\text{--}150 \text{ mg L}^{-1}$. A 2.0 mmol L^{-1} KMnO_4 was used as a colorimetric reagent for cinnarizine determination by dissolving 0.0316 g of KMnO_4 in 100 mL of 1.0 mol L^{-1} H_2SO_4 .

The univariate optimization method was used to study the effect of various parameters and identify the optimal condition by considering sensitivity and linearity. A series of standard solutions of cinnarizine at $1, 10, 25, 50, 100$, and 150 mg L^{-1} in 0.1 mol L^{-1} HCl was tested under initial conditions which included a flow rate of 1.0 mL min^{-1} and 10 cm of injection loop with 2.0 mmol L^{-1} KMnO_4 in 0.5 mol L^{-1} sulfuric acid. Both physical and chemical parameters such as flow rate ($0.4\text{--}1.0 \text{ mL min}^{-1}$), injection volume ($10\text{--}20 \mu\text{L}$), concentrations of KMnO_4 ($0.1\text{--}2.5 \text{ mmol L}^{-1}$) and H_2SO_4 ($0.1\text{--}1.5 \text{ mol L}^{-1}$) were investigated.

Eleven brands of cinnarizine tablets were purchased from drugstores in Bangkok, Thailand. Twenty tablets of each brand were weighed and finely powdered, and a portion equivalent to 25 mg of cinnarizine was transferred to a 100.0 mL volumetric flask and dissolved in 0.1 mol L^{-1} hydrochloric acid; then the mixture was sonicated for 10 min to dissolve the active ingredient. After that, the samples were filtered through a Whatman No. 1 paper filter and 10.0 mL of filtrate was diluted to 50.0 mL with 0.1 mol L^{-1} of hydrochloric acid. These sample solutions were analyzed by the proposed system and the results compared using high performance liquid chromatography (HPLC) (LC-20AP, Shimadzu, Japan) with Diode Array Detection (SPD-M20A, Shimadzu, Japan). The system included an Inertsil ODS-3 C18 column ($4.6 \times 250 \text{ mm}$, $5 \mu\text{m}$) with guard column Inertsil ODS-3 ($4.6 \times 10 \text{ mm}$, $5 \mu\text{m}$), at a flow rate of 1.2 mL min^{-1} and injection volume of $20 \mu\text{L}$, with detection at 250 nm . The mobile phase

consisted of acetate buffer pH4:methanol ($30:70$) [37].

3. Results and Discussion

3.1 Application for phosphate analysis

3D LOC incorporating r-FIA was applied to determine PO_4^{3-} based on PMB reaction. However, the optimization is necessary to achieve a good analytical feature. The signal in absorbance value (after subtraction of the blank peak) was used for the determination of PO_4^{3-} .

3.1.1 Optimization for PO_4^{3-} Analysis

The univariate optimization was used to study the effect of some chemical and physical parameters to determine the concentration of phosphate that can be related to the absorption of PMB complex. The influence of flow rate within the range of 0.8 to 1.5 mL min^{-1} was examined using a PO_4^{3-} standard solution of 1.0 mg P L^{-1} . The findings indicate that higher flow rates resulted in reducing signal intensity due to the rapid flow (Fig. 3a). In the PMB reaction, ascorbic acid served as a reductant, requiring time to reduce 12-PMA to form the blue PMB complex. Although the flow rate of 0.8 mL min^{-1} gave a little higher sensitivity than that of 1.0 mL min^{-1} , the low flow rate increased run time. Therefore, compromising the analysis time and sensitivity, a flow rate of 1.0 mL min^{-1} was selected for further experiments.

As mentioned by Nagul et al. [35], the acid and molybdate concentrations are preponderant, not only for the formation of the heteropoly acid, but also for controlling its reduction. Therefore, concentration of H_2SO_4 and molybdate were the first two chemical parameters to study for optimization. H_2SO_4 effect was investigated in the range of 2 to 8 mol L^{-1} . The results show that at 4 mol L^{-1} presented the highest signal (Fig. 3b). At this concentration of H_2SO_4 , the pH of combined reagent was about 1 , and when the reagent was injected in the PO_4^{3-} stream, the pH affected the formation of phosphomolybdate species and its reduction to form deep blue complex [35].

However, at 1 mol L⁻¹ H₂SO₄, the combined reagent presented blue color and the reagent was not stable; therefore, no result of this concentration is presented in the graph. Divya et al. [38] also reported that the blue complex by molybdenum can be formed at low H⁺ level even in the absence of PO₄³⁻.

The effect of molybdenum concentration was also studied in the range of 1-50 mmol L⁻¹ (Fig. 3c). It was observed that the signal increased as the concentration of ammonium molybdate increased, reaching a maximum at 10.0 mmol L⁻¹ and declining after this concentration. The presence of excess concentrations of ammonium molybdate resulted in the development of a more intense yellow color of the blank. Therefore, 10.0 mmol L⁻¹ of ammonium molybdate was chosen.

Antimony tartrate played a crucial role in enhancing the rate of reduction with ascorbic

acid. So, various concentrations of antimony tartrate were studied at 2, 4, 6, 8 and 10 mmol L⁻¹; and the results presented the signal of 0.3013 ± 0.0009 , 0.3154 ± 0.0026 , 0.3209 ± 0.0010 , 0.3216 ± 0.0003 and 0.3223 ± 0.0006 , respectively. There is almost no difference in the signal of each concentration. The concentration of 8.0 mmol L⁻¹ was selected because it presented the lowest standard deviation. Lastly, ascorbic acid was employed to reduce molybdophosphate, resulting in the formation of the blue PMB complex. The concentration of ascorbic acid was studied in the range of 0.1 to 1.0 mol L⁻¹ (Fig. 3d). Results indicated that an increasing concentration of ascorbic acid led to higher absorbance. However, it was noted that the blank signal increased significantly when ascorbic acid was higher than 0.5 mol L⁻¹, causing a decrease in the signal of the analyte.

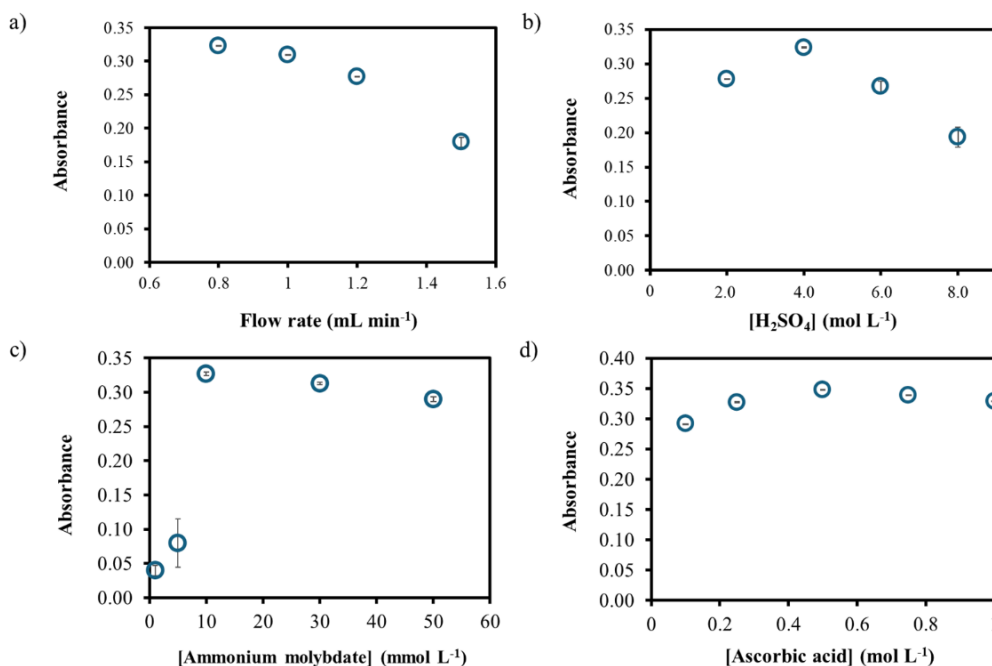


Fig. 3. The optimal condition of 3D LOC coupled with r-FIA system for phosphate determination, a) Effect of flow rate (mL min⁻¹); b) [Sulfuric acid, H₂SO₄] (mol L⁻¹); c) [Ammonium molybdate] (mmol L⁻¹); and d) [Ascorbic acid] (mol L⁻¹).

In summary, the optimal conditions for the combined reagent consisted of 4 mol L⁻¹ H₂SO₄, 10.0 mmol L⁻¹ of ammonium

molybdate, 8.0 mmol L⁻¹ of antimony tartrate and 0.5 mol L⁻¹ of ascorbic acid, and the flow rate of r-FIA system was 1.0 mL min⁻¹.

3.1.2 Analytical performance of PO_4^{3-}

Under the optimal conditions, a linear calibration was proceeded in the range of 0.010–2.0 mg P L⁻¹. The linear equation describing the relationship between absorbance signal value (y) and phosphate concentration (x) in unit of mg P L⁻¹ is represented as $y = 0.3085x - 0.0074$ with R^2 value of 0.9985. The limit of detection and quantitation (LOD and LOQ) were calculated based on three times and ten times the standard deviation of the blank. For the proposed method, the LOD and LOQ were found to be 0.003 mg P L⁻¹ and 0.010 mg P L⁻¹, respectively. The precision of PO_4^{3-} standard solution at 1.0 mg P L⁻¹ was investigated both with 10-replicate injections and 10 bottles of solution, and the results showed % RSD of 1.02 and 1.32, respectively. To assess the recovery of this method, the standard phosphate at four different levels;

0.010, 0.10, 0.50, and 1.0 mg P L⁻¹; were spiked into the sample solution and the percent recoveries were found at 95.0 ± 3.2 , 98.0 ± 1.2 , 94.5 ± 0.6 and 94.6 ± 0.6 , respectively. The proposed method yielded good recoveries indicating its suitability for determining phosphate concentration in the surface water samples with sample throughput of 40 h⁻¹.

Furthermore, comparing the analytical characteristics of the proposed method with those of other methods that employ the molybdenum blue reaction for determination of phosphate in water samples, a summary of working range and LOD has been presented in Table 1. Literatures indicate that there are several reports for determination of phosphate in water samples based on the PMB method. However, the method developed in this research demonstrates a lower detection limit compared to the batch method using UV-visible spectrophotometers [39–41]. Although

Table 1. Comparison of the proposed method with some recent publications for phosphate detection based on the PMB method in natural water samples.

| System | Sample | Detection wavelength (nm) | Linearity range (mg PL ⁻¹) | LOD (mg PL ⁻¹) | Ref. |
|--|--|---------------------------|--|----------------------------|------------------|
| UV-visible spectrophotometer | Sugarcane Juice, Fertilizer, Detergent and Water Samples | 840 nm | 0.1–11 | – | [39] |
| UV-Visible Spectroscopy | Natural water | 890 nm | 0.1–1 | – | [40] |
| UV-Visible Spectroscopy | Surface water | 700 nm | – | 0.006 | [41] |
| r-FIA with spectrophotometer | Estuarine waters | 880 nm | 0.002–0.1 | 0.002 | [42] |
| Lab-on-a-disc with colorimetric detection | River water | 880 nm | 0.014–0.8 | 0.005 | [43] |
| Programmable flow injection with spectrophotometer | Seawater | 880 nm | 0–0.076 | – | [25] |
| UV-Visible Spectroscopy | Natural Water and Detergent Samples | 870 nm | 0.05–9 | 0.18 | [44] |
| 3D LOC with r-FIA | Natural water | 880 nm | 0.01–2.0 | 0.003 | This work |

the proposed method has a higher limit of LOD than flow injection analysis, it offers a wider working range and is superior in terms of reducing sample and reagent volume

consumption. Additionally, it allows for semi-automated operation, making it suitable for analyzing phosphate in natural water samples.

3.1.3 Interference study

Interference in the phosphomolybdic acid method, often referred to as the molybdenum blue method, for phosphate determination can arise from various ions. The molybdenum blue method relies on the formation of a blue-colored complex between phosphomolybdic acid and reducing agents, such as ascorbic acid, in the presence of phosphate. In this section, the interference study of this system was carried out by examining the reaction of phosphate with ammonium molybdate in the presence of various anions and metal ions commonly found in natural water. The evaluated ions included Cu^{2+} , Zn^{2+} , Mn^{2+} , Fe^{3+} , Al^{3+} , Ca^{2+} , Mg^{2+} , K^+ , NH_4^+ , Cl^- , NO_3^- and SO_4^{2-} . This study aimed to determine if these ions might interact or interfere with the phosphate detection process. To investigate potential interference, various interfering ions were introduced into a 0.5 mg P L^{-1} standard phosphate solution. Specifically, 10.0 mg L^{-1} of Cu^{2+} , Zn^{2+} , Mn^{2+} , Fe^{3+} and Al^{3+} (representing metal ions), as well as 100.0 mg L^{-1} Ca^{2+} and Mg^{2+} and $1,000.0 \text{ mg L}^{-1}$ K^+ , NH_4^+ , Cl^- , NO_3^- and SO_4^{2-} were added. The signal of each solution of PO_4^{3-} with and without adding other ions is presented in Fig. 4. The relative error of each solution that added Cu^{2+} , Zn^{2+} , Mn^{2+} , Fe^{3+} , Al^{3+} , Ca^{2+} , Mg^{2+} , K^+ , NH_4^+ , Cl^- , NO_3^- and SO_4^{2-} was found to be 1.90, 0.53, 1.07, 3.57, 0.56, 0.83, 0.94, 1.43, 1.15, 2.16, 3.87 and 6.22, respectively. The result indicates that the addition of these ions did not affect the analyte signal, with an inaccuracy of less than 5%. While the presence of SO_4^{2-} did slightly impact the phosphate signal, with an inaccuracy greater than 5% but less than 10%, attributed to antimony present in the combined reagents. Jonge et al. [45] mentioned that the interaction between antimony and sulfide resulted in the forming of SbS , leading to a replacement of the PMB spectra by the spectrum of phosphomolybdenum-antimony blue. This issue can be addressed by using a higher antimony concentration in the method.

However, the concentrations of these ions in the study exceeded the permissible levels in water sources. According to the U.S. Environmental Protection Agency (USEPA), the maximum allowable contaminant levels for Cu^{2+} , Zn^{2+} , Mn^{2+} , Fe^{3+} , Al^{3+} , Ca^{2+} , Mg^{2+} , NH_4^+ , Cl^- , NO_3^- and SO_4^{2-} in natural water is 1.3, 5, 0.05, 0.3, 0.2, 100, 60, 35, 32.5, 250, 10 and 250 mg L^{-1} , respectively [20, 46]. Overall, these ions did not significantly affect the outcomes of this study.

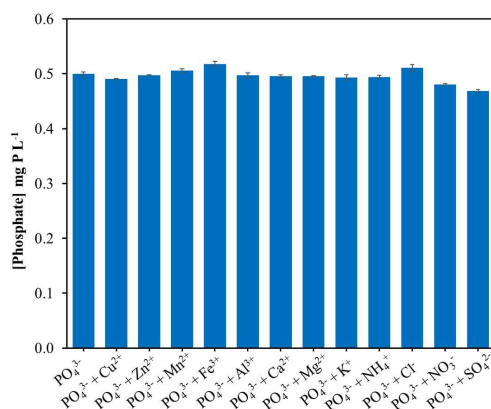


Fig. 4. Effect of interferences on phosphate determination.

3.1.4 Phosphate determination in water samples

Phosphate determination in water samples is essential for assessing water quality, as phosphates can contribute to eutrophication and algae blooms in aquatic ecosystems. The amounts of PO_4^{3-} in 10 surface water samples in Thammasat University Rangsit campus (including lake and canal) were analyzed by the proposed method and the conventional batch method (PMB method) [36]. The findings revealed that the phosphate concentration in all samples was below 0.10 mg P L^{-1} except for sample 2, as illustrated in Fig. 5. Importantly, statistical analysis using a paired t-test at a 95% confidence level indicated that there was no significant difference between the results obtained by the two methods, with a t-statistic of 1.80 and a critical t-value of 2.26. In 1986, the Environmental Protection Agency (EPA)

established the recommended criteria for phosphorus such as not more than 0.05 and 0.1 mg L⁻¹ for streams discharging into reservoirs, and streams that do not empty into reservoirs, respectively, that aimed at controlling eutrophication in natural water [20]. However, sample 2 exhibited a phosphate content exceeding this limit. This case may be attributed to the leaching of fertilizer into water sources or the discharge of wastewater from buildings into the water. These results suggest that the proposed method is successful and effective in determining of phosphate levels in water samples.

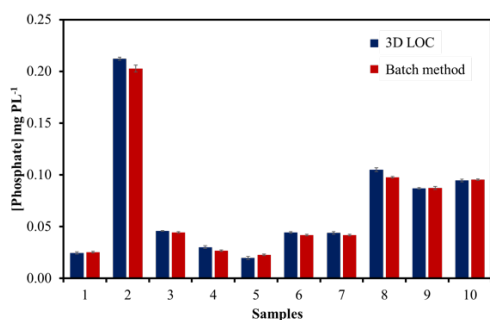


Fig. 5. Determination of phosphate content in natural water with the proposed method and the batch method.

3.2 Application for cinnarizine analysis

This method was based on the oxidation reaction of cinnarizine by KMnO₄ in an acidic solution [33], leading to the dark purple color of KMnO₄ fade. The absorption spectra of 2.0 mmol L⁻¹ KMnO₄ in 0.1 mol L⁻¹ H₂SO₄ was measured by scanning the spectra using a UV-Vis spectrophotometer (UV-1700, Shimadzu, Japan) in the range 300-800 nm and the maximum absorbance was found at 525 nm. After adding cinnarizine (10 mg L⁻¹) to KMnO₄, the absorbance at this wavelength decreased as shown in Fig. 6.

The 3D LOC was incorporated into r-FIA and spectrophotometry to determine cinnarizine by monitoring the decreasing intensity color of KMnO₄ at 525 nm. The standard cinnarizine (or sample solution) was propelled by peristaltic pump into the system

(Fig. 2) and the KMnO₄ in an acidic solution was injected by the six-port valve and then flowed into the stream of cinnarizine solution and 3D LOC for reaction; after that, the peak was observed. The FIAGram was plotted between absorbance vs. time (sec). However, the signal for determination of cinnarizine was calculated in percentage of decolorization ($(1 - A_1/A_0) \times 100$), whereas A_0 is peak height of KMnO₄ in blank stream (0.1 mol L⁻¹ HCl), and A_1 is those of KMnO₄ in cinnarizine stream.

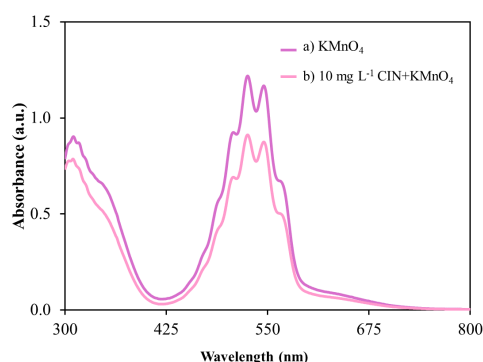


Fig. 6. The absorption spectra of a) KMnO₄ in acidic solution and b) 10 mg L⁻¹ Cinnarizine in KMnO₄ solution.

3.2.1 Optimization of cinnarizine system

The effect of physical and chemical variables on the performance of the method was studied. The starting condition used standard solutions of cinnarizine at 1, 10, 25, 50, 100, and 150 mg L⁻¹ in 0.1 mol L⁻¹ HCl, at a flow rate of 1.0 mL min⁻¹, injection loop of 10 µL with 2.0 mmol L⁻¹ KMnO₄ in 0.5 mol L⁻¹ sulfuric acid. The optimal condition was selected by considering of linearity ($R^2 \geq 0.99$) and sensitivity (slope) of each parameter.

The flow rate of the peristaltic pump was investigated in the range 0.4-1.0 mL min⁻¹ (Fig. 7a)). Increasing the flow rate, the higher linearity was observed, in contrast to the sensitivity. The flow rate affected both the reaction and mixing capacity; the best linearity was found at flow rate of 0.8 mL min⁻¹ (with $R^2 > 0.99$); therefore, this condition was selected for further studies. The injection volumes of 10.0 and 20.0 µL were

studied; 20 μL of KMnO_4 were used in the next study because it presented good linearity (R^2 0.9944.).

Next, the effect of concentrations of permanganate was studied in the range of 0.1-2.5 mmol L^{-1} in 0.5 mol L^{-1} sulfuric acid (Fig. 7b). At higher concentration of KMnO_4 , the better linearity was obtained until at 2.0 mmol L^{-1} , when in contrast, the lower sensitivity was presented. We suggest that higher concentrations of permanganate caused the detector to receive low intensity of light. The result of 2.0 mmol L^{-1} KMnO_4 , gave the best compromise between sensitivity and linearity.

Sulfuric acid acts as a catalyst in the oxidation reaction of permanganate. Its concentrations were studied in the range 0.1-1.5 mol L^{-1} , as shown in Fig. 7c. The highest linearity was obtained at 0.5 and 1.0 mol L^{-1} . The optimal condition was 1.0 mol L^{-1} of sulfuric acid, as this gave the highest slope with R^2 greater than 0.99. The optimized condition was 20 μL of 2.0 mmol L^{-1} of permanganate in a 1.0 mol L^{-1} of sulfuric acid as the reagent, and 0.8 mL min^{-1} flow rate; and it was used throughout the experiments.

3.2.2 Analytical performance of cinarrizine determination

Under the optimal conditions, a calibration graph was presented by plotting the percent decolorization of permanganate against the concentration of cinarrizine standard (mg L^{-1}). The FIAGram (absorbance vs. time (sec)) is shown in Fig. 8. As the concentration of cinarrizine increased, the peak height decreased because the cinarrizine was oxidized by permanganate; hence, fading of permanganate color resulted. This method offered a linear calibration in the range 10-150 mg L^{-1} and the linear equations of % decolorization = $0.5253 [\text{cinarrizine}] + 8.0135$ with R^2 0.9963 ($n = 3$). The limit of detection and quantitation (LOD and LOQ)

were calculated following the ICH guideline criteria, as 3SD and 10SD, respectively, where SD is the standard deviation of the blank measurements. The LOD and LOQ of the proposed method were 2.5 mg L^{-1} and 8.0 mg L^{-1} , respectively. A 10-replicate injection of permanganate into a stream of 50.0 mg L^{-1} of cinarrizine standard was done. The percent relative standard deviation (% RSD) was 2.2. Moreover, ten solutions at 50.0 mg L^{-1} of cinarrizine were analyzed in 3-replicate injections of permanganate solution, and % RSD was 3.5. To study the recovery of this method, five concentrations of cinarrizine at 5, 10, 15, 20 and 25 mg L^{-1} were spiked into the sample; the percentage recoveries were found to be 101.8, 98.0, 97.5, 96.3 and 98.2, respectively.

In this section, 3D LOC coupled to r-FIA was applied to determine cinarrizine in tablets dosage form based on oxidation reaction by KMnO_4 in acidic medium. A comprehensive comparison of the analytical performance between our proposed system and previous methods for cinarrizine determination in pharmaceutical dosage forms has been summarized in Table 2. Although chromatography remains an official assay for cinarrizine analysis as specified in the British Pharmacopoeia 2020 [34], it has limitations of long analysis time, the use of organic solvents, and expensive instrumentation.

Therefore, there are alternative developments of the analysis of cinarrizine in tablets dosage form, including UV-vis spectrophotometry [31, 32], colorimetry [49-51], and flow injection analysis [33]. Although the 3D coupled with r-FIA provided worse LOD than others, it is still suitable for the assay of cinarrizine in pharmaceuticals without the complicated sample preparation process. Moreover, it is superior in terms of Green Analytical Chemistry because it involves low reagent consumption and less hazardous

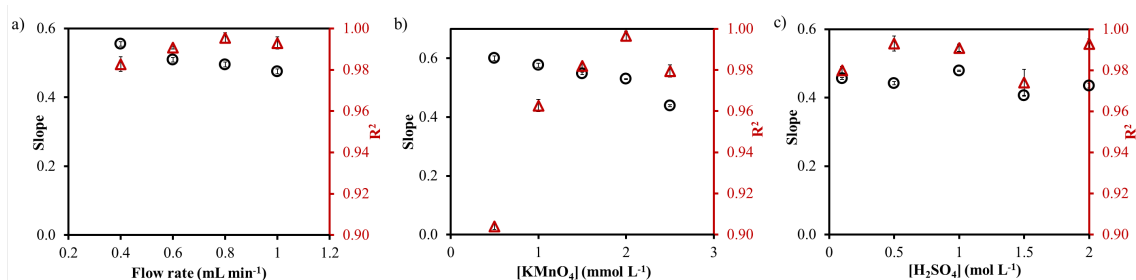


Fig. 7. The optimization study of 3D LOC coupled with r-FIA system for determination of cinnarizine, a) Effect of flow rate (mL min^{-1}); b) $[\text{KMnO}_4]$ (mmol L^{-1}); and c) $[\text{H}_2\text{SO}_4]$ (mol L^{-1}) in the system.

Table 2. Comparison methods for determination of cinnarizine in pharmaceutical dosage forms.

| System | Condition | Linearity range (mg L^{-1}) | LOD (mg L^{-1}) | Ref. |
|----------------------------|---|--|----------------------------|------------------|
| RP-HPLC | Column: MICRA-NPS C18 Mobile phase: acetonitrile: triethylamine buffer: THF (30:66:4) Flow rate: 0.5 mL min^{-1} . Wavelength: 253 nm | 0.02–0.1 | 5.92×10^{-5} | [47] |
| RP-HPLC | Column: C8 Mobile phase: 0.05 M KH_2PO_4 (pH3): methanol (35:65) Flow rate: 1.0 mL min^{-1} . Wavelength: 253 nm | 2–20 | 0.527 | [48] |
| RP-HPLC | Column: RP-C18 Mobile phase: acetonitrile: 0.1% SLS in water (90:10) Flow rate: 2.0 mL min^{-1} . Wavelength: 215 nm | 1–25 | 0.05 | [27] |
| LC-MS/MS | Column: Atlantis d C18 Mobile phase: Trifluoroacetic acid and acetonitrile (0.1:100) Flow rate: 1.0 mL min^{-1} . | – | 0.49 | [28] |
| UV spectrophotometry | Solvent: Methanol Wavelength: 253 nm | 5–30 | 0.0389 | [31] |
| UV spectrophotometry | Solvent: Methanol Wavelength: 250 nm | 4–20 | – | [32] |
| Colorimetry | Reagent: Bromocresol green, Bromocresol purple, Bromocresol blue Solvent: chloroform Wavelength: 414 nm | 2–10 | 0.63 | [49] |
| Colorimetry | Reagent: 3-Methyl-benzothiazoline-2-one and FeCl_3 Solvent: HCl Wavelength: 630 nm | 10–40 | 2 | [50] |
| Colorimetry | Reagent Dipicrylamine Solvent: Ethyl acetate and CHCl_3 Wavelength: 402.8 nm | 1.5–36.8 | 0.40 | [51] |
| FIA with Chemiluminescence | Reagent: $7.5 \times 10^{-4} \text{ M KMnO}_4$ in 0.02 M PPA and 10%v/v ethanol in $1.5 \times 10^{-3} \text{ M Tween 60}$ Flow rate: 7.6 mL min^{-1} | 0.5–6.0 | 0.018 | [33] |
| 3D LOC with r-FIA | Reagent: 2.0 mM KMnO_4 in 1.0 M H_2SO_4 Flow rate: 0.8 mL min⁻¹ Wavelength: 550 nm | 10.0–150.0 | 2.5 | This work |

chemicals than other colorimetric reagents. FIA-chemiluminescence [33] applied a high flow rate for achieving higher sample throughput (198 samples per hour) than the proposed method (60 samples per hour); however, the 3D LOC system provided a wider linearity range.

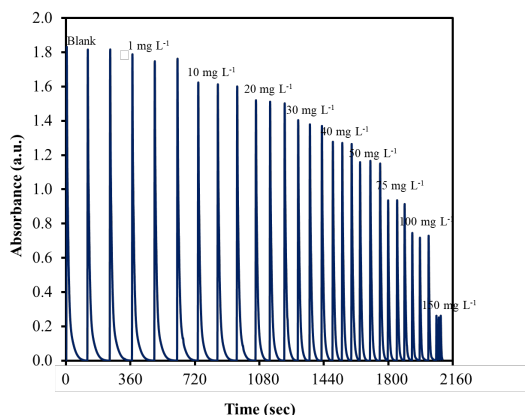


Fig. 8. FIAgram for cinnarizine 0-150 mg L⁻¹.

3.3.3 Cinnarizine assays in tablet dosage form

The proposed method was applied to determine cinnarizine in tablet dosage form of 11 brands that are distributed in Thailand. The label of each sample listed 25 mg of cinnarizine per tablet. The results obtained by the proposed methods were compared to the HPLC method [35], as shown in Fig. 9.

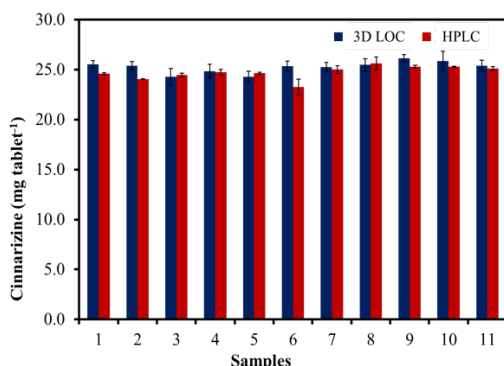


Fig. 9. Comparison of cinnarizine content found by the proposed method and HPLC method

The results showed that there is no significant difference between the two methods at 95% confidence level with

t-statistic value of 1.95 and t-critical of 2.23. Moreover, the assays of cinnarizine for 11 brands of samples are in the range of 24.3-25.8 mg per tablet or 97.2-103.2 % labelled amount (% LA), which met the requirement of BP 2020 (95.0-105.0 % LA) [34]. Therefore, the proposed method may be an alternative method for determining the cinnarizine formulation with the sample throughput 60 samples per hour.

4. Conclusions

Herein, the three-dimension lab on a chip (3D LOD) integrated with reverse flow injection analysis (r-FIA) was successful for determining cinnarizine in tablet dosage form and phosphate in water samples based on colorimetric detection. The 3D LOC was fabricated for a novel microchannel network that acted as a micro-reaction coil in a flow-through-cell. The dimensions are 12x10x45 mm, similar to a conventional cuvette or flow-through cell used in flow-based analysis, compatible with general spectrophotometers. The proposed system represents a novel and alternative approach for the flow-based system with colorimetric detection, offering greener analytical methods by minimizing reagent consumption and waste generation, while using common reagents that are less hazardous than traditional colorimetric reagents.

Acknowledgements

This study was supported by Thammasat University Research Fund Contract No. TUFT 023/2563. The authors would like to acknowledge the Department of Chemistry, Faculty of Science and Technology, Thammasat University for supporting laboratory facilities, and thanks to Thammasat University Center of Scientific Equipment for Advanced Research (TUCSEAR). In addition, N. Siangdee greatly thanks the Science Achievement Scholarships of Thailand (SAST) for financial support for her PhD study.

References

- [1] Saroj S, Priya S, Vinod J, Rajeshwari R. Green analytical chemistry and quality by design: a combined approach towards robust and sustainable modern analysis. *Current Analytical Chemistry*, 2017;13(4).
- [2] Venkatesan K, Sundarababu J, Anandan S. The recent developments of green and sustainable chemistry in multidimensional way: current trends and challenges. *Green Chemistry Letters and Reviews*, 2024;17(1):2312848.
- [3] Nunes JK, Stone HA. Stone, Introduction: microfluidics. *Chemical Reviews*, 2022; 122(7):6919-20.
- [4] Sonnen KF, Merten CA. Microfluidics as an emerging precision tool in developmental biology. *Developmental Cell*, 2019;48(3):293-311.
- [5] Rawas-Qalaji M, Cagliani R, Al-hashini N, Al-Dabbagh R, Al-Dabbagh A, Hussain Z. Microfluidics in drug delivery: review of methods and applications. *Pharmaceutical Development and Technology*, 2023; 28(1):61-77.
- [6] Thimmaraju M M, Trivedi R, Hemalatha G, Thirupathy B, Billah A M. Microfluidic revolution and its impact on pharmaceutical materials: A review. *Materials Today: Proceedings*, 2023.
- [7] Gharib G, Butun I, Muganli Z, Kozalak G, Namli I, Sarraf SS, Ahmadi VE, Toyran E, Wijnen AJ, Kosar A. Biomedical applications of microfluidic devices: a review. *Biosensors*, 2022;12:1023.
- [8] Aryal P, Hefner C, Martinez B, Henry CS. Microfluidics in environmental analysis: advancements, challenges, and future prospects for rapid and efficient monitoring. *Lab on a Chip*, 2024;24:1175-1206.
- [9] Mesquita P, Gong L, Lin Y. Low-cost microfluidics: towards affordable environmental monitoring and assessment. *Frontiers in Lab on a Chip Technologies*, 2022;1:1074009.
- [10] Jang Y-H, Hancock MJ, Kim SB, Selimovic S, Sim WY, Bae H, Khademhosseini A. An integrated microfluidic device for two-dimensional combinatorial dilution. *Lab on a Chip*, 2011;11(19):3277-86.
- [11] Wang Y, Sun S, Luo J, Xiong Y, Ming T, Liu J, Ma Y, Yan S, Yang Y, Yang Z, Reboud J, Yin H, cooper JM, Cai X. Low sample volume origami-paper-based graphene-modified aptasensors for label-free electrochemical detection of cancer biomarker-EGFR. *Microsystems & Nanoengineering*, 2020;6(1):32.
- [12] Massimiani A, Panini F, Marasso SL, Cocuzza M. 2D Microfluidic Devices for Pore-Scale Phenomena Investigation: A Review. *Water*, 2023;15(6):1222.
- [13] Qi W, Zheng L, Wang S, Huang F, Liu Y, Jiang H, Lin J. A microfluidic biosensor for rapid and automatic detection of Salmonella using metal-organic framework and Raspberry Pi. *Biosensors and Bioelectronics*, 2021;178:113020.
- [14] Cao Q, Liang B, Tu T, Wei J, Fang L, Ye X. Three-dimensional paper-based microfluidic electrochemical integrated devices (3D-PMED) for wearable electrochemical glucose detection. *RSC Advances*, 2019;9(10):5674-81.
- [15] Zhang Y. Three-dimensional-printing for microfluidics or the other way around? *International Journal of Bioprinting*, 2019; 5(2):192.
- [16] Gupta V, Paull B. PolyJet printed high aspect ratio three-dimensional bifurcating microfluidic flow distributor and its application in solid-phase extraction. *Analytica Chimica Acta*, 2021;1168: 338624.
- [17] Khot MI, Levenstein MA, Boer GN, Armstrong G, Maisey T, Svavarsdottir HS, Andrew H, Perry SL, Kapur N, Jayne DG.

- Characterising a PDMS based 3D cell culturing microfluidic platform for screening chemotherapeutic drug cytotoxic activity. *Scientific Reports*, 2020;10(1):15915.
- [18] Tarn MD, Pamme N. *Microfluidics*. 2013. p. 1-7.
- [19] Li X, Fan X, Li Z, Shi L, Liu J, Luo H, Wang L, Du X, Chen W, Guo J, Li C, Liu S. Application of Microfluidics in Drug Development from Traditional Medicine. *Biosensors*, 2022;12(10):870.
- [20] U.S. Environmental Protection Agency, 1986, Quality criteria for water 1986: Washington, D.C., U.S. Environmental Protection Agency Report 440/5-86-001, Office of Water.
- [21] Worsfold P, McKelvie I, Monbet P. Determination of phosphorus in natural waters: A historical review. *Analytica Chimica Acta*, 2016;918:8-20.
- [22] Manzoori JL, Miyazaki A, Tao H. Rapid differential flow injection of phosphorus compounds in wastewater by sequential spectrophotometry and inductively coupled plasma atomic emission spectrometry using a vacuum ultraviolet emission line. *Analyst*, 1990;115(8):1055-8.
- [23] Taniai T, Sukegawa M, Sakuragawa A, Uzawa A. On-line preconcentration of phosphate onto molybdate form anion exchange column. *Talanta*, 2003;61(6): 905-12.
- [24] Kröckel L, Lehmann H, Wieduwilt T, Schmidt MA. Fluorescence detection for phosphate monitoring using reverse injection analysis. *Talanta*, 2014;125:107-13.
- [25] Hatta M, ruzicka J, Measures C, Davis M. Automated calibration by a single standard solution prepared in deionized water by flow programming eliminates the schlieren and salinity effects and is applied to the determination of phosphate in sea water of different salinities. *Talanta*, 2022;253:124041.
- [26] Sereenonchai K, Inla C, Buajarern S. Thread-Based Analytical Device for Determination of Phosphorus Content in Fertilizers. *Trends in Sciences*, 2022;19: 5616.
- [27] Edrees FH, Saad AS, Alsaadi T, Amin NH. Experimentally designed chromatographic method for the simultaneous analysis of dimenhydrinate, cinnarizine and their toxic impurities. *RSC Advances*, 2021;11(3): 1450-60.
- [28] Mullangi S, Ravindhranath K, Yarala MR, Panchakarla RK. A sensitive LC-MS/MS method for the determination of potential genotoxic impurities in Cinnarizine. *Annales Pharmaceutiques Françaises*, 2023;81(1):74-82.
- [29] Alqarni MH, Shakeel F, Foudah AI, Aljarba T. A Validated, Stability-Indicating, Eco-Friendly HPTLC Method for the Determination of Cinnarizine. *Separations*, 2023;10:138.
- [30] El-Houssini OM, Mohammad MA. Versatile TLC-densitometric methods for the synchronous estimation of cinnarizine and acefylline heptaminol in the presence of potential impurity and their reported degradation products. *Journal of Chromatographic Science*, 2022;60(9): 832-9.
- [31] Kalyankar TM, Wadher SJ, Kulkarni PD, Panchakshari PP. Simultaneous estimation and development of UV spectroscopic method for determination of cinnarizine and domperidone in bulk and pharmaceutical formulation. *International Journal of PharmTech Research*, 2014;6(1):323-9.
- [32] Lamie NT. Comparative study of spectrophotometric methods manipulating ratio spectra: an application on pharmaceutical binary mixture of cinnarizine and dimenhydrinate. *Spectrochimica Acta Part A: Molecular*

- and Biomolecular Spectroscopy, 2015; 141:193-201.
- [33] Townshend A, Youngvises N, Wheatley RA, Liawruangrath S. Flow-injection determination of cinnarizine using surfactant-enhanced permanganate chemiluminescence. *Analytica Chimica Acta*, 2003;499(1):223-33.
- [34] British Pharmacopoeia. 2020. London: Station Office Ltd.
- [35] Nagul EA, McKelvie ID, Worsfold P, Kolev SD. The molybdenum blue reaction for the determination of orthophosphate revisited: Opening the black box. *Analytica Chimica Acta*, 2015;890:60-82.
- [36] Cheewasedtham W, Sirikarn J, Rujiralai T. Simple spectrophotometric determination of phosphate in concentrated latex. *European Journal of Scientific Research*, 2012;81(3):408-16.
- [37] Hassan SSM, Elmosallamy MAF, Abbas AB. LC and TLC determination of cinnarizine in pharmaceutical preparations and serum. *Journal of Pharmaceutical and Biomedical Analysis*, 2002;28(3):711-9.
- [38] Divya S, Sharmila P, Dinakaran J, Yamal G, Rao KS, Pardha-Saradhi P. Specific H^+ level is crucial for accurate phosphate quantification using ascorbate as a reductant. *Protoplasma*, 2020;257(1):319-30.
- [39] Pradhan S, Pokhrel MR. Spectrophotometric Determination of Phosphate in Sugarcane Juice, Fertilizer, Detergent and Water Samples by Molybdenum Blue Method. *Scientific World*, 2013;(11)11:58-62.
- [40] Habibah N, Dhyana Putri IGAS, Karta IWW, Sundari CDWH, Hadi MC. A simple spectrophotometric method for the quantitative analysis of phosphate in the water samples. *JST (Journal Sains dan Teknologi)*, 2018;7(2):198.
- [41] Lin B, Xu J, Yin C, Chen L, You Y, Hu L. An ultraviolet dual-wavelength and dual-beam chemical sensor on small UAV for in-situ determination of phosphate and nitrite in surface water. *Sensors and Actuators B: Chemical*, 2022;368: 132235.
- [42] Auflitsch S, Peat DMW, Worsfold PJ, Auflitsch S, McKelvie LD. Determination of dissolved reactive phosphorus in estuarine waters using a reversed flow injection manifold. *Analyst*, 1997;122(12): 1477-80.
- [43] Duffy G, Maguire I, Heery B, Nwankire C, Ducree J, Regan F. PhosphaSense: A fully integrated, portable lab-on-a-disc device for phosphate determination in water. *Sensors and Actuators B: Chemical*, 2017; 246:1085-91.
- [44] Ismail VS. The Blue Molybdenum Reaction for the Determination of Phosphate in Natural Water and Detergent Samples. *Journal of University of Babylon for Pure and Applied Sciences*, 2023;31(3):10-25.
- [45] De Jonge VN, Villerius LA, Interference of sulphide in inorganic phosphate determination in natural waters. *Marine Chemistry*, 1980;9(3):191-7.
- [46] Driscoll DG, Carter JM, Williamson JE, Putnam LD. *Hydrology of the Black Hills Area*, South Dakota. 2002.
- [47] Heda AA, sonawane AR, Naranje GH, PURANIK PK. A Rapid Determination of cinnarizine in bulk a pharmaceutical dosage form by LC. *Journal of Chemistry*, 2010;7(3):1080-4.
- [48] Ahmed AB, Abdelwahab NS, Abdelrahman MM, Salama FM. Simultaneous determination of dimenhydrinate, cinnarizine and cinnarizine impurity by TLC and HPLC chromatographic methods. *Bulletin of Faculty of Pharmacy, Cairo University*, 2017;55(1):163-9.

- [49] Abdine H, Belal F, Zoman N. Simple spectrophotometric determination of cinnarizine in its dosage forms. *Il Farmaco*, 2002;57(4):267-71.
- [50] Metwally F, El-Zeiny B, Darwish H. New Methods for Determination of Cinnarizine in Mixture with Piracetam by Spectrodensitometry, Spectrophotometry, and Liquid Chromatography. *Journal of AOAC International*, 2005;88:1666-76.
- [51] Issa Y, Youssef A, El-Hawary WF, Abdel-Ghaffar E, Spectrophotometric determination of cinnarizine through charge-transfer complex formation with polynitro compounds. *European Chemical Bulletin*, 2013;2(7):507-15.